

Low–high voltage duality in tunneling spectroscopy of the Sachdev-Ye-Kitaev model

N. V. Gnedilov, J. A. Hutasoit, and C. W. J. Beenakker

Instituut-Lorentz, Universiteit Leiden, P.O. Box 9506, 2300 RA Leiden, The Netherlands

(Dated: July 2018)

The Sachdev-Ye-Kitaev (SYK) model describes a strongly correlated metal with all-to-all random interactions (average strength J) between N fermions (complex Dirac fermions or real Majorana fermions). In the large- N limit a conformal symmetry emerges that renders the model exactly soluble. Here we study how the non-Fermi liquid behavior of the closed system in equilibrium manifests itself in an open system out of equilibrium. We calculate the current-voltage characteristic of a quantum dot, described by the complex-valued SYK model, coupled to a voltage source via a single-channel metallic lead (coupling strength Γ). A one-parameter scaling law appears in the large- N conformal regime, where the differential conductance $G = dI/dV$ depends on the applied voltage only through the dimensionless combination $\xi = eVJ/\Gamma^2$. Low and high voltages are related by the duality $G(\xi) = G(\pi/\xi)$. This provides for an unambiguous signature of the conformal symmetry in tunneling spectroscopy.

Introduction — The Sachdev-Ye-Kitaev model, a fermionic version¹ of a disordered quantum Heisenberg magnet,^{2,3} describes how N fermionic zero-energy modes are broadened into a band of width J by random infinite-range interactions. The phase diagram of the SYK Hamiltonian can be solved exactly in the large- N limit,^{4–6} when a conformal symmetry emerges at low energies that forms a holographic description of the horizon of an extremal black hole in a (1+1)-dimensional anti-de Sitter space.^{1,3,4,7}

To be able to probe this holographic behaviour in the laboratory, it is of interest to create a “black hole on a chip”,^{8–10} that is, to realize the SYK model in the solid state. Ref. 8 proposed to use a quantum dot formed by an opening in a superconducting sheet on the surface of a topological insulator. In a perpendicular magnetic field the quantum dot can trap vortices, each of which contains a Majorana zero-mode.¹¹ Chiral symmetry ensures that the band only broadens as a result of four-Majorana-fermion terms in the Hamiltonian, a prerequisite for the real-valued SYK model. A similar construction uses an array of Majorana nanowires coupled to a quantum dot.⁹ Since it might be easier to start from conventional electrons rather than Majorana fermions, Ref. 10 suggested to work with the complex-valued SYK model of interacting Dirac fermions in the zeroth Landau level of a graphene quantum dot. Chiral symmetry at the charge-neutrality point again suppresses broadening of the band by two-fermion terms.

The natural way to study a quantum dot is via transport properties. Electrical conduction through chains of SYK quantum dots has been studied in Refs. 12–19. For a single quantum dot coupled to a tunnel contact, as in Fig. 1, Refs. 8–10 studied the limit of negligibly small coupling strength Γ , in which the differential conductance $G = dI/dV$ equals the density of states of the quantum dot. Conformal symmetry in the large- N limit gives a low-voltage divergence $\propto 1/\sqrt{V}$, until eV drops below the single-particle level spacing $\delta \simeq J/N$.^{20–22}

Here we investigate how a finite Γ affects the tunneling spectroscopy. We focus on the complex-valued SYK

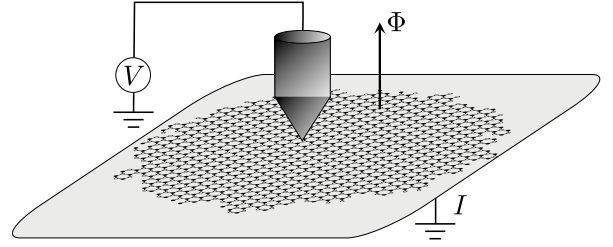


FIG. 1: Tunneling spectroscopy of a graphene flake, in order to probe the complex-valued SYK model.¹⁰ We calculate the current I driven by a voltage V through a single-channel point contact (coupling strength Γ) into a graphene flake on a grounded conducting substrate. At the charge neutrality point a chiral symmetry ensures that the zeroth Landau level (degeneracy $N = e\Phi/h$ for an enclosed flux Φ) is only broadened by electron-electron interactions (strength J). For a sufficiently random boundary the quantum dot can be described by the SYK Hamiltonian (1).

model for Dirac fermions, as in the graphene quantum dot of Ref. 10. Our key result is that in the large- N conformal symmetry regime $J/N \ll eV \ll J$ the zero-temperature differential conductance of the quantum dot depends on Γ , J , and V only via the dimensionless combination $\xi = eVJ/\Gamma^2$. Low and high voltages are related by the duality $G(\xi) = G(\pi/\xi)$, providing an experimental signature of the conformal symmetry.

Tunneling Hamiltonian — We describe the geometry of Fig. 1 by the Hamiltonian

$$\begin{aligned}
 H &= H_{\text{SYK}} + \sum_p \varepsilon_p \psi_p^\dagger \psi_p + \sum_{i,p} (\lambda_i c_i^\dagger \psi_p + \lambda_i^* \psi_p^\dagger c_i), \\
 H_{\text{SYK}} &= (2N)^{-3/2} \sum_{ijkl} J_{ij;kl} c_i^\dagger c_j^\dagger c_k c_l, \\
 J_{ij;kl} &= J_{kl;ij}^* = -J_{ji;kl} = -J_{ij;lk}.
 \end{aligned} \tag{1}$$

The annihilation operators c_i , $i = 1, 2, \dots$ represent the $N = h\Phi/e$ interacting Dirac fermions in the spin-polarized zeroth Landau level of the graphene quantum dot (enclosing a flux Φ). Two-fermion terms $c_i^\dagger c_j$ are suppressed by chiral symmetry when the Fermi level $\mu = 0$ is

at the charge-neutrality point (Dirac point).¹⁰ The operators ψ_p represent electrons at momentum p in the single-channel lead (dispersion $\varepsilon_p = p^2/2m$, linearized near the Fermi level), coupled to mode i in the quantum dot with complex amplitude λ_i . The tunneling current depends only on the sum of $|\lambda_i|^2$, via the coupling strength

$$\Gamma = \pi \rho_{\text{lead}} \sum_i |\lambda_i|^2, \quad \rho_{\text{lead}} = (2\pi \hbar v_F)^{-1}. \quad (2)$$

If $\mathcal{T} \in (0, 1)$ is the transmission probability into the quantum dot, one has $\Gamma \simeq \mathcal{T} N \delta \simeq \mathcal{T} J$.

The Hamiltonian H_{SYK} is the complex-valued SYK model⁴ if we take random couplings $J_{ij;kl}$ that are independently distributed Gaussians with zero mean $\langle J_{ij;kl} \rangle = 0$ and variance $\langle |J_{ij;kl}|^2 \rangle = J^2$. The zeroth Landau level then broadens into a band of width J , corresponding to a single-particle level spacing $\delta \simeq J/N$ (more precisely, $\delta \simeq J/N \ln N$).²⁰ In the energy range $\delta \ll \varepsilon \ll J$ the retarded Green's functions can be evaluated in saddle-point approximation,⁴

$$G^{\text{R}}(\varepsilon) = -i\pi^{1/4} \sqrt{\frac{\beta}{2\pi J}} \frac{\Gamma(1/4 - i\beta\varepsilon/2\pi)}{\Gamma(3/4 - i\beta\varepsilon/2\pi)}, \quad (3)$$

where $\beta = 1/k_B T$ and $\Gamma(x)$ is the Gamma function. At zero temperature this simplifies to

$$G^{\text{R}}(\varepsilon) = -i\pi^{1/4} \exp\left[\frac{1}{4}i\pi \operatorname{sgn}(\varepsilon)\right] |\varepsilon|^{-1/2}. \quad (4)$$

Quantum fluctuations around the saddle point cut off the low- ε divergence for $|\varepsilon| < \delta$.²⁰⁻²²

Tunneling current — The quantum dot is strongly coupled to a grounded substrate,²³ so the current is entirely determined by the transmission of electrons through the point contact. The current operator \mathbf{I} is given by the commutator

$$\mathbf{I} = \frac{ie}{\hbar} \left[H, \sum_p \psi_p^\dagger \psi_p \right] = i \frac{e}{\hbar} \sum_{n,p} (\lambda_n c_n^\dagger \psi_p - \lambda_n^* \psi_p^\dagger c_n). \quad (5)$$

We calculate the time-averaged expectation value of \mathbf{I} using the Keldysh path integral technique,²⁴⁻²⁷ which has previously been applied to the SYK model in Refs. 12, 14, 18, 28. The expectation value I of the tunneling current is given by the first derivative of cumulant generating function:²⁵

$$I = -i \lim_{\chi \rightarrow 0} \frac{\partial}{\partial \chi} \ln Z(\chi), \quad (6)$$

$$Z(\chi) = \langle \mathcal{T}_C \exp(-i \int_C dt [H + \frac{1}{2} \chi(t) \mathbf{I}]) \rangle. \quad (7)$$

Here \mathcal{T}_C indicates time-ordering along the Keldysh contour²⁴ of the counting field $\chi(t)$, equal to $+\chi$ on the forward branch of the contour (from $t = 0$ to $t = \infty$) and equal to $-\chi$ on the backward branch (from $t = \infty$ to $t = 0$). The calculation is worked out in the Appendix.

The result for the differential conductance is

$$G = \frac{dI}{dV} = \frac{e^2}{h} \int_{-\infty}^{+\infty} d\varepsilon f'(\varepsilon - eV) \frac{4\Gamma \operatorname{Im} G^{\text{R}}(\varepsilon)}{|1 + i\Gamma G^{\text{R}}(\varepsilon)|^2}, \quad (8)$$

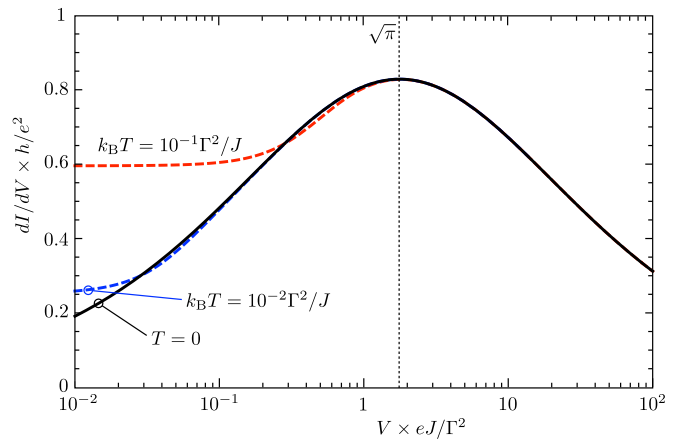


FIG. 2: Differential conductance $G = dI/dV$ calculated from Eq. (8), as a function of dimensionless voltage $\xi = eVJ/\Gamma^2$ for three different temperatures. On the semi-logarithmic scale the duality between low and high voltages shows up as a reflection symmetry along the dotted line (where $\xi = \sqrt{\pi}$).

where $f(\varepsilon) = (1 + e^{\beta\varepsilon})^{-1}$ is the Fermi function. Substitution of the conformal Green's function (3) gives upon integration the finite temperature curves plotted in Fig. 2.

At zero temperature $f'(\varepsilon - eV) \rightarrow -\delta(\varepsilon - eV)$ and substitution of Eq. (4) produces a single-parameter function of $\xi = eVJ/\Gamma^2$,

$$G(\xi) = \frac{e^2}{h} \frac{2\sqrt{2}}{\sqrt{2} + \pi^{1/4} \xi^{-1/2} + \pi^{-1/4} \xi^{1/2}}. \quad (9)$$

Low-high voltage duality — The $T = 0$ differential conductance (9) in the conformal regime $J/N \ll eV \ll J$ satisfies the duality relation

$$G(\xi) = G(\pi/\xi), \quad \text{if } N^{-1}(J/\Gamma)^2 \ll \xi, 1/\xi \ll (J/\Gamma)^2. \quad (10)$$

The V -to- $1/V$ duality is visible in the semi-logarithmic Fig. 2 by a reflection symmetry of the differential conductance along the $\xi = \sqrt{\pi}$ axis. The symmetry is precise at $T = 0$, and is broken in the tails with increasing temperature.

The voltage range in which V and $1/V$ are related by Eq. (10) covers the full conformal regime for $N \simeq (J/\Gamma)^4$. In this voltage range the $1/\sqrt{V}$ tail at high voltages crosses over to a \sqrt{V} decay at low voltages. The high-voltage tail reproduces the $1/\sqrt{V}$ differential conductance that follows⁸⁻¹⁰ from the density of states in the limit $\Gamma \rightarrow 0$ (since $\xi \rightarrow \infty$ for $\Gamma \rightarrow 0$). The density of states gives²⁰⁻²² a crossover to a \sqrt{V} decay when eV drops below the single-particle level spacing $\delta \simeq J/N$. Our finite- Γ result (9) implies that this crossover already sets in at larger voltages $eV \simeq \Gamma^2/J$, well above δ for $N \gg (J/\Gamma)^2$.

The symmetrically peaked profile of Fig. 2 is a signature of conformal symmetry in as much as this produces a power-law singularity in the retarded propagator at low

energies. It is not specific for the square-root singularity (4), other exponents would give a qualitatively similar low-high voltage duality. For example, the generalized SYK_{2p} model with $2p \geq 4$ interacting Majorana fermion terms has a $\varepsilon^{(1-p)/p}$ singularity,^{5,13} corresponding to the duality $G(\xi_p) = G(C_p/\xi_p)$ with C_p a numerical coefficient and $\xi_p = (eV)^{2(p-1)/p} J^{2/p} \Gamma^{-2}$. In contrast, a disordered Fermi liquid such as the non-interacting SYK₂ model, with Hamiltonian $H = \sum_{ij} J_{ij} c_i^\dagger c_j$, has a constant propagator at low energies and hence a constant dI/dV in the range $J/N \ll eV \ll J$.

Conclusion — We have shown that tunneling spectroscopy can reveal a low–high voltage duality in the conformal regime of the Sachdev-Ye-Kitaev model of N interacting Dirac fermions. A physical system in which one might search for this duality is the graphene quantum dot in the lowest Landau level, proposed by Chen, Ilan, De Juan, Pikulin, and Franz.¹⁰

As argued by those authors, one should be able to reach N of order 10^2 for laboratory magnetic field strengths in a sub-micrometer-size quantum dot. This leaves two decades in the conformal regime $J/N \ll eV \ll J$. If we tune the tunnel coupling strength near the ballistic limit $\Gamma \lesssim J$, it should be possible even for these moderately large values of N to achieve $N \simeq (J/\Gamma)^4$ and access the duality over two decades of voltage variation. For such large Γ the condition on temperature, $k_B T \ll \Gamma^2/J$ would then also be within experimental reach ($J \simeq 34$ meV from Ref. 10 and $\Gamma \simeq 10$ meV has $k_B T = 10^{-2} \Gamma^2/J$ at $T = 300$ mK).

Acknowledgements — We have benefited from discussions with K. E. Schalm and A. Romero Bermudez. This research was supported by the Netherlands Organization for Scientific Research (NWO/OCW) and by an ERC Synergy Grant.

Appendix A: Outline of the calculation

We describe the calculation leading to Eq. (8) for the current-voltage characteristics, generalizing it to nonzero chemical potential μ and including also the shot noise power. We set \hbar and e to unity, except for the final formulas.

1. Generating function of counting statistics

Arbitrary cumulants of the current operator (5) can be obtained from the generating function (7). A gauge transformation allows us to write equivalently

$$Z(\chi) = \langle \mathcal{T}_C \exp(-i \int_C H(t) dt) \rangle, \quad (\text{A1})$$

$$H(t) = H_{\text{SYK}} + \sum_p \varepsilon_p \psi_p^\dagger \psi_p - \mu \sum_n c_n^\dagger c_n + \sum_{n,p} (e^{i\chi(t)/2} \lambda_n c_n^\dagger \psi_p + e^{-i\chi(t)/2} \lambda_n^* \psi_p^\dagger c_n). \quad (\text{A2})$$

For generality we have added a chemical potential term $\propto \mu$. (In the main text we take $\mu = 0$, corresponding to a quantum dot at charge neutrality.)

We need the advanced and retarded Green's functions

$G^A(\varepsilon) = (G^R(\varepsilon))^*$ and the Keldysh Green's function

$$G^K(\varepsilon) = \mathcal{F}(\varepsilon) (G^R(\varepsilon) - G^A(\varepsilon)), \quad \mathcal{F}(\varepsilon) = \tanh(\beta\varepsilon/2). \quad (\text{A3})$$

These are collected in the matrix Green's function \mathcal{G} , which on the Keldysh contour has the representation^{26,27,29}

$$\mathcal{G} = \begin{pmatrix} G^R & G^K \\ 0 & G^A \end{pmatrix} = L \sigma_3 \begin{pmatrix} G^{++} & G^{+-} \\ G^{-+} & G^{--} \end{pmatrix} L^\dagger, \quad (\text{A4})$$

$$L = \frac{1}{\sqrt{2}} \begin{pmatrix} 1 & -1 \\ 1 & 1 \end{pmatrix}, \quad \sigma_3 = \begin{pmatrix} 1 & 0 \\ 0 & -1 \end{pmatrix}, \quad (\text{A5})$$

in terms of the Green's functions on the forward and backward branches of the contour:

$$G^{++}(t, t') = -iN^{-1} \sum_n \langle \mathcal{T} c_n(t) c_n^\dagger(t') \rangle, \quad (\text{A6a})$$

$$G^{+-}(t, t') = iN^{-1} \sum_n \langle c_n^\dagger(t') c_n(t) \rangle, \quad (\text{A6b})$$

$$G^{-+}(t, t') = -iN^{-1} \sum_n \langle c_n(t) c_n^\dagger(t') \rangle, \quad (\text{A6c})$$

$$G^{--}(t, t') = -iN^{-1} \sum_n \langle \mathcal{T}^{-1} c_n(t) c_n^\dagger(t') \rangle. \quad (\text{A6d})$$

The operators \mathcal{T} and \mathcal{T}^{-1} order the times in increasing and decreasing order, respectively.

2. Saddle point solution

In the regime $J/N \ll \varepsilon \ll J$ the Green's function of the SYK model is given by the saddle point solution⁴

$$G^R(\varepsilon) = -iC e^{-i\theta} \sqrt{\frac{\beta}{2\pi J}} \frac{\Gamma\left(\frac{1}{4} - i\frac{\beta\varepsilon}{2\pi} + i\varepsilon\right)}{\Gamma\left(\frac{3}{4} - i\frac{\beta\varepsilon}{2\pi} + i\varepsilon\right)}, \quad (\text{A7})$$

with the definitions

$$e^{2\pi\varepsilon} = \frac{\sin\left(\frac{\pi}{4} + \theta\right)}{\sin\left(\frac{\pi}{4} - \theta\right)}, \quad C = (\pi/\cos 2\theta)^{1/4}. \quad (\text{A8})$$

The angle $\theta \in (-\pi/4, \pi/4)$ is a spectral asymmetry angle,³⁰ determined by the charge per site $\mathcal{Q} \in (-1/2, 1/2)$ on the quantum dot according to³¹

$$\mathcal{Q} = N^{-1} \sum_i \langle c_i^\dagger c_i \rangle - \frac{1}{2} = -\theta/\pi - \frac{1}{4} \sin 2\theta. \quad (\text{A9})$$

For $\mu = 0$, when $\mathcal{Q} = 0$, one has $\theta = 0$, $C = \pi^{1/4}$. In good approximation (accurate within 15%),

$$\theta \approx -\frac{1}{2}\pi\mathcal{Q} \Rightarrow C \approx (\pi/\cos \pi\mathcal{Q})^{1/4}. \quad (\text{A10})$$

In the mean-field approach the quartic SYK interaction (1) is replaced by a quadratic one with the kernel \mathcal{G}^{-1} from Eq. (A4). A Gaussian integration over the Grassmann fields gives the generating function

$$\ln Z = \int_{-\infty}^{\infty} \frac{d\varepsilon}{2\pi} \ln \left(\frac{\det [1 - \Gamma \Xi(\varepsilon) \Lambda^\dagger \mathcal{G}(\varepsilon) \Lambda]}{\det [1 - \Gamma \Xi(\varepsilon) \mathcal{G}(\varepsilon)]} \right), \quad \Lambda = \begin{pmatrix} \cos(\chi/2) & i \sin(\chi/2) \\ i \sin(\chi/2) & \cos(\chi/2) \end{pmatrix}, \quad \Xi(\varepsilon) = -i \begin{pmatrix} 1 & 2\mathcal{F}(\varepsilon - V) \\ 0 & -1 \end{pmatrix}. \quad (\text{A11})$$

The matrix $\Xi(\varepsilon)$ is the Keldysh Green's function of the lead, integrated over the momenta. This evaluates further to

$$\ln Z = \int_{-\infty}^{\infty} \frac{d\varepsilon}{2\pi} \ln \left[1 + \frac{i\Gamma(G^R - G^A)}{(1 + i\Gamma G^R)(1 - i\Gamma G^A)} \left([1 - \mathcal{F}(\varepsilon)\mathcal{F}(\varepsilon - V)](\cos \chi - 1) + i[\mathcal{F}(\varepsilon) - \mathcal{F}(\varepsilon - V)] \sin \chi \right) \right]. \quad (\text{A12})$$

At zero temperature the distribution function simplifies to $\mathcal{F}(\varepsilon) \mapsto \text{sgn}(\varepsilon)$, hence

$$\ln Z = \int_0^V \frac{d\varepsilon}{2\pi} \ln \left[1 + \frac{2i\Gamma(G^R - G^A)(e^{i\varepsilon} - 1)}{(1 + i\Gamma G^R)(1 - i\Gamma G^A)} \right]. \quad (\text{A13})$$

3. Average current and shot noise power

A p -fold differentiation of $Z(\chi)$ with respect to χ gives the p -th cumulant of the current. In this way the full counting statistics of the charge transmitted through the quantum dot can be calculated.²⁵ The first cumulant, the time-averaged current I from Eq. (6), is given by

$$I = \frac{e}{h} \int_{-\infty}^{+\infty} d\varepsilon \frac{i\Gamma[\mathcal{F}(\varepsilon) - \mathcal{F}(\varepsilon - V)](G^R - G^A)}{(1 + i\Gamma G^R)(1 - i\Gamma G^A)}, \quad (\text{A14})$$

which is Eq. (8) from the main text.

At zero temperature the differential conductance $G = dI/dV$ is

$$G(\xi) = \frac{2e^2}{h} \left[1 + \frac{1}{2 \sin(\pi/4 + \theta)} \left(\frac{\sqrt{\xi}}{C} + \frac{C}{\sqrt{\xi}} \right) \right]^{-1}, \quad (\text{A15})$$

with $\xi = eVJ/\Gamma^2$. The duality relation

$$G(\xi) = G(C^4/\xi) \quad (\text{A16})$$

reduces to the one from the main text, $G(\xi) = G(\pi/\xi)$, when we set $\mu = 0 \Rightarrow \theta = 0 \Rightarrow C = \pi^{1/4}$.

The second cumulant, the shot noise power P , follows similarly from

$$P = - \lim_{\chi \rightarrow 0} \frac{\partial^2}{\partial \chi^2} \ln Z(\chi). \quad (\text{A17})$$

The Fano factor F , being the ratio of the shot noise power and the current at zero temperature, is simply given by

$$F = \frac{dP/dV}{dI/dV} = e \left(1 - \frac{h}{e^2} G \right). \quad (\text{A18})$$

It has the same one-parameter scaling and duality as G . The fact that higher order cumulants of the current have the same scaling as the differential conductance is a consequence of the single-point-contact geometry, with a single counting field $\chi(t)$. This does not carry over to a two-point-contact geometry.

¹ A. Kitaev, *A simple model of quantum holography*, KITP Program: Entanglement in Strongly-Correlated Quantum Matter, April 7 and May 27, 2015.

² S. Sachdev and J. Ye, *Gapless spin-fluid ground state in a random quantum Heisenberg magnet*, Phys. Rev. Lett. **70**, 3339 (1993).

³ S. Sachdev, *Holographic metals and the fractionalized Fermi liquid*, Phys. Rev. Lett. **105**, 151602 (2010).

⁴ S. Sachdev, *Bekenstein-Hawking entropy and strange metals*, Phys. Rev. X **5**, 041025 (2015).

⁵ J. Maldacena and D. Stanford, *Remarks on the Sachdev-Ye-Kitaev model*, Phys. Rev. D **94**, 106002 (2016).

⁶ J. Polchinski and V. Rosenhaus, *The spectrum in the Sachdev-Ye-Kitaev model*, JHEP **04**, 1 (2016).

⁷ A. Kitaev and S. J. Suh, *The soft mode in the Sachdev-Ye-Kitaev model and its gravity dual*, JHEP **05**, 183 (2018).

⁸ D. I. Pikulin and M. Franz, *Black hole on a chip: proposal for a physical realization of the SYK model in a solid-state system*, Phys. Rev. X **7**, 031006 (2017).

⁹ A. Chew, A. Essin, and J. Alicea, *Approximating the Sachdev-Ye-Kitaev model with Majorana wires*, Phys. Rev. B **96**, 121119(R) (2017).

¹⁰ A. Chen, R. Ilan, F. de Juan, D. I. Pikulin, and M. Franz, *Quantum holography in a graphene flake with an irregular boundary*, Phys. Rev. Lett. **121**, 036403 (2018).

¹¹ L. Fu and C. L. Kane, *Superconducting proximity effect and Majorana fermions at the surface of a topological insulator*, Phys. Rev. Lett. **100**, 096407 (2008).

¹² X.-Y. Song, C.-M. Jian, and L. Balents, *Strongly correlated metal built from Sachdev-Ye-Kitaev models*, Phys. Rev. Lett. **119**, 216601 (2017).

¹³ R. A. Davison, W. Fu, A. Georges, Y. Gu, K. Jensen, and

- S. Sachdev, *Thermoelectric transport in disordered metals without quasiparticles: The Sachdev-Ye-Kitaev models and holography*, Phys. Rev. B **95**, 155131 (2017).
- ¹⁴ P. Zhang, *Dispersive SYK model: band structure and quantum chaos*, Phys. Rev. B **96**, 205138 (2017).
- ¹⁵ Y. Gu, X.-L. Qi, and D. Stanford, *Local criticality, diffusion and chaos in generalized Sachdev-Ye-Kitaev models*, JHEP **05**, 125 (2017).
- ¹⁶ Xin Chen, Ruihua Fan, Yiming Chen, Hui Zhai, and Pengfei Zhang, *Competition between chaotic and non-chaotic phases in a quadratically coupled Sachdev-Ye-Kitaev model*, Phys. Rev. Lett. **119**, 207603 (2017).
- ¹⁷ D. Ben-Zion and J. McGreevy, *Strange metal from local quantum chaos*, Phys. Rev. B **97**, 155117 (2018).
- ¹⁸ A. Haldar, S. Banerjee, and V. B. Shenoy, *Higher-dimensional SYK non-Fermi liquids at Lifshitz transitions*, Phys. Rev. B **97**, 241106 (2018).
- ¹⁹ Y. Zhong, *Periodic Anderson model meets Sachdev-Ye-Kitaev interaction: A solvable playground for heavy fermion physics*, arXiv:1803.09417
- ²⁰ D. Bagrets, A. Altland, and A. Kamenev, *Sachdev-Ye-Kitaev model as Liouville quantum mechanics*, Nucl. Phys. B **911**, 191 (2016).
- ²¹ D. Bagrets, A. Altland, A. Kamenev, *Power-law out of time order correlation functions in the SYK model*, Nucl. Phys. B **921**, 727 (2017).
- ²² A. V. Lunkin, K. S. Tikhonov, and M. V. Feigel'man, *SYK model with quadratic perturbations: the route to a non-Fermi-liquid*, arXiv:1806.11211.
- ²³ We assume that the grounded substrate does not spoil the non-Fermi liquid state of the quantum dot. This might happen if the coupling becomes too strong, according to S. Banerjee and E. Altman, *Solvable model for a dynamical quantum phase transition from fast to slow scrambling*, Phys. Rev. B **95**, 134302 (2017).
- ²⁴ L. V. Keldysh, *Diagram technique for nonequilibrium processes*, JETP **20**, 4, p. 1018 (1965).
- ²⁵ L. S. Levitov, H.-W. Lee, and G. B. Lesovik, *Electron counting statistics and coherent states of electric current*, Journal of Mathematical Physics **37**, 4845 (1996).
- ²⁶ A. Kamenev and A. Levchenko, *Keldysh technique and non-linear σ -model: basic principles and applications*, Adv. in Physics **58**, 197 (2009).
- ²⁷ A. Kamenev, *Field Theory of Non-Equilibrium Systems* (Cambridge University Press, 2011).
- ²⁸ A. Eberlein, V. Kasper, S. Sachdev, and J. Steinberg, *Quantum quench of the Sachdev-Ye-Kitaev Model*, Phys. Rev. B **96**, 205123 (2017).
- ²⁹ A. I. Larkin and Yu. N. Ovchinnikov, *Nonlinear conductivity of superconductors in the mixed state*, JETP **41**, 960 (1975).
- ³⁰ O. Parcollet, A. Georges, G. Kotliar, and A. Sengupta, *Overscreened multichannel $SU(N)$ Kondo model: Large- N solution and conformal field theory*, Phys. Rev. B **58**, 3794 (1998).
- ³¹ A. Georges, O. Parcollet, and S. Sachdev, *Quantum fluctuations of a nearly critical Heisenberg spin glass*, Phys. Rev. B **63**, 134406 (2001).